

ACTIVE REGION BLINKERS: TRANSIENT EVENTS IN THE SOLAR ATMOSPHERE

R.W. Walsh¹, J. Ireland¹, R.A. Harrison², E.R. Priest¹¹ School of Mathematical and Computational Sciences, University of St. Andrews, KY16 9SS, U.K.² Space Science Department, Rutherford Appleton Laboratory, Chilton, Didcot, Oxfordshire, OX11 0QX, U.K.

ABSTRACT

As part of the St. Andrews/RAL Loops Campaign, the NIS instrument on CDS was used to study a small active region between 14th and 15th November 1996. High cadence observations over a wide range of temperatures reveal many examples of temporally well-defined, localised increases in intensity in the brightest regions. This is particularly the case for the transition region line (O V 629.73Å). Two such events are presented here that show a substantial increase in emission.

It is found that these impulsive events effect the plasma temperature over two orders of magnitude (chromospheric to coronal), the event lifetimes being hundreds of seconds. The calculated Doppler velocities range from 30 to 70 km s⁻¹ in O V 629.73Å, comparable with blinkers. Also, there is an apparent line broadening connected with the events. The fact that the brightenings enhance the emission in coronal lines (up to 2.5×10^6 K) presents the possibility that these type of transient phenomena could be observed by SXT on Yohkoh. A crude calculation of the thermal energy content suggests that these events may be indicative of low energy, discrete heating in the corona, the energy released being of the order of 10^{24} erg.

Key words: active regions, transient events, EUV Sun.

1. INTRODUCTION

One of the main aims of the SOHO Mission is further our understanding on how the solar corona is heated. Many mechanisms have been suggested in the literature as candidates, and many reviews exist outlining specific heating mechanisms in some detail (for example, Narain and Ulmschneider 1990 and Zirker 1993). Recently, much interest has centred on the suggestion that the necessary energy deposition is due to many discrete, random heating bursts. This is largely motivated by Parker (1988), who suggested that a large number of low energy events (10^{24} erg per

event), termed nanoflares could provide enough energy to heat the corona. Nanoflares are the result of magnetic reconnection at the braided boundaries of twisted flux tubes that have their photospheric footpoints subjected to bounded, continuous displacement and shuffling. Since then, several authors have modelled the effect of these transient events on coronal plasma (see Kopp and Poletto, 1993; Cargill 1994; Vlahos *et al* 1995; Walsh, Bell and Hood 1997).

Various names have been given to what appear to be a wide range of possible transient phenomena in the solar atmosphere: microflares (Moore *et al* 1994; Schmieder *et al* 1994; Porter, Fontenla and Simnett 1995), active region transient brightenings (Shimizu 1995), explosive events (Dere 1994; Innes *et al* 1997) and blinkers (Harrison 1997; Brekke, Fludra and Harrison 1997) to name but a few.

Table 1 contains the average duration, lengthscale of energy release, energy content, possible Doppler velocities and frequency of occurrence for the above mentioned events, in comparison with the two events studied in this paper. It should be noted that in this paper, the authors define a micro (nano)flare as an event that releases 10^{27} (10^{24})erg in some event lifetime.

2. THE ST. ANDREWS/RAL LOOPS CAMPAIGN

The findings described below form part of a series of observations taken with CDS on 12th-15th November, 1996. Two observing sequences were used, EJECT_V3 (version 18) and LOOPS_3 (version 1). EJECT_V3 was used in this campaign to take a snapshot of the region of interest before and after multiple runs of the higher cadence, smaller area LOOPS_3 study. This latter study is designed to look for rapid variations in active regions and takes one image approximately every 14 seconds. A summary description of LOOPS_3 and EJECT_V3 are given in Table 2 and Table 3.

A typical run of the campaign would involved running EJECT_V3 initially to provide some density diagnostics and an image of the region of interest. Then LOOPS_3 is run, perhaps a few times, on one of several specific points of interest in that region, say at

Event	D (s)	L (Mm)	E (erg)	DV (km s ⁻¹)	F (s ⁻¹)
Blinkers					
Harrison (1997)	300	18	4.4×10^{25}	35-45	11
Brekke <i>et al</i> (1997)	180-1800	-	-	-	-
Explosive Events					
Dere (1994)	60	1.5	-	150	600
Innes <i>et al</i> (1997)	240	12-24	-	100	-
Micro/Nanoflares					
Parker (1988)	20	2	10^{24}	-	-
Moore <i>et al</i> (1994)	180	-	10^{27}	-	-
Schmieder <i>et al</i> (1994)	360	6	10^{28}	-	-
Porter <i>et al</i> (1995)	60	2-10	10^{27}	-	-
ARTB					
Schimizu (1995)	120 - 420	0.5 - 4	$10^{25} - 10^{29}$	-	-
Event1					
He I	600	14	3×10^{27}	24-34	-
O V	600	14	3×10^{25}	35-65	-
Mg IX	300	6	2×10^{24}	20?	-
Fe XVI	300	5	3×10^{24}	20?	-
Event2					
He I	800	18	6×10^{27}	28-38	-
O V	1000	18	6×10^{25}	52-72	-
Mg IX	-	-	-	-	-
Fe XVI	-	-	-	-	-

Table 1. Characteristics of the wide range of small-scale transient phenomena observed in the corona (including the events observed within this LOOPS_3 study) for approximate duration (D), lengthscale (L), energy released (E), calculated Doppler velocities (DV) and frequency of occurrence (F) of the events over the full disk.

Table 2. EJECT_V3 observing sequence.

Instrument	CDS-NIS, $4 \times 240\text{arcsec}^2$ slit
Locations	60, at 4 arcsec steps, total area, $240 \times 240\text{arcsec}^2$
Duration	10s per location, 991s for complete sequence.
Lines	He I 584.33Å, O V 629.73Å, Mg IX 368.06Å, Fe XVI 360.76Å Si10 347.4Å Si10 356.04Å

Table 3. LOOPS_3 observing sequence.

Instrument	CDS-NIS, $4 \times 240\text{arcsec}^2$ slit
Locations	1, total area $4 \times 120\text{arcsec}^2$
Duration	10s per location, 707s for a complete sequence of 50 rasters.
Lines	He I 584.33Å, Mg IX 368.06Å, O V 629.73Å, Fe XVI 360.76Å

suspected coronal loop footprints. To close the campaign, EJECT_V3 is run again to determine if any overall changes in the region of interest have occurred while LOOPS_3 has been running.

3. Results

The results presented below were obtained from data taken on the 15th November 1996 of an active region present in the south-east quadrant of the Sun. An EJECT_V3 run was taken to start the sequence. This was followed by nine LOOPS_3 runs in three blocks

of three. The first block (stored as CDS FITS files labelled s5762r00,01,02) was positioned over a region of positive magnetic flux, as observed with the Michelson Doppler Interferometer (MDI) on board SoHO. Similarly, the third block (CDS FITS s5764r00,01,02) of LOOPS_3 runs was placed over the corresponding negative magnetic flux region. The intermediate block was placed between the flux regions (CDS FITS s5763r00,01,02). Each block of three LOOPS_3 runs forms a long duration, high cadence set of observations over physically different parts of an active region. A figure showing the slit positions over the emerging active region can be found in these proceedings in Ireland, Walsh, Harrison and Priest 1997 where results of time series analysis are investigated.

There are many examples in the LOOPS_3 data of temporally well-defined, localised increases in the brightest regions observed. This is particularly the case for the O V line. These brightenings may be due to the presence of transient energy events. Generally it is difficult to single out a specific event within these bright regions. However, two events in the data have been found to show a substantial increase in intensity and can be isolated to some degree, since they are obviously distinct from their surroundings as seen in the data.

3.1. Event 1 (s5764 data)

About 1100s into the run, a significant localised increase in intensity is observed in the southernmost quarter of the slit (pixels 55 to 70) (see Figure 1 for He I and O V). It occurs within a bright region in all the lines and Figure 2 shows the temporal variation of this particular region where the “background” intensity at time=1100s has been subtracted. The width

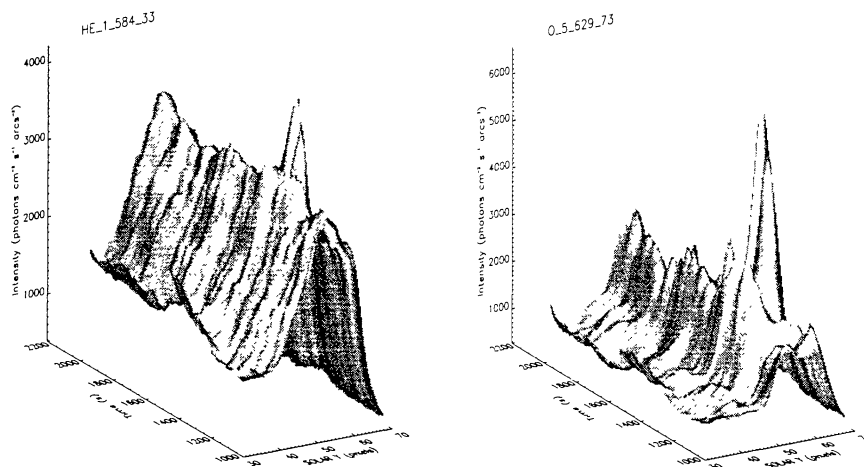


Figure 1. Event 1: temporal variation along the slit for lines He I and O V in data s5764.

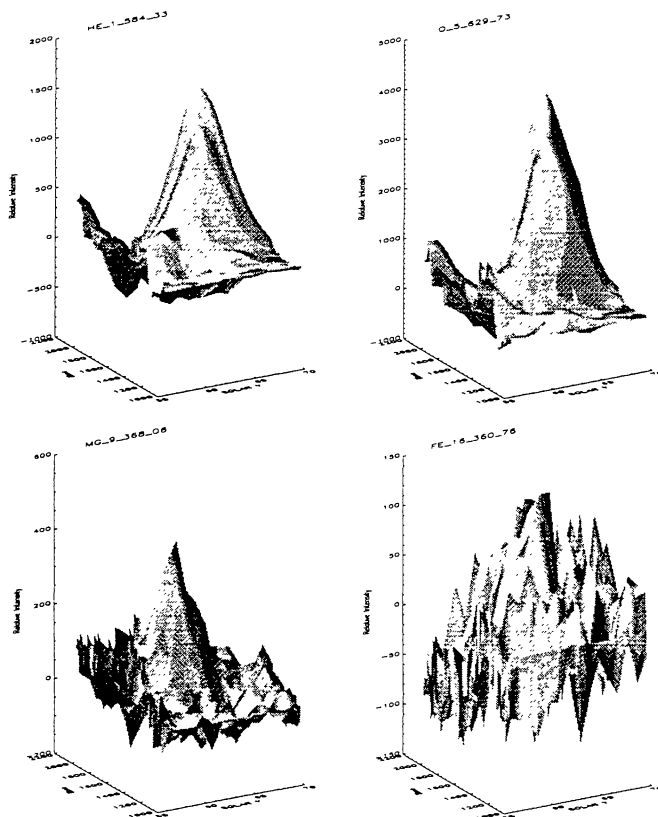


Figure 2. Event 1: change in intensity ($\text{photons cm}^{-2} \text{s}^{-1} \text{arcsecs}^{-2}$) for all lines relative to intensity at time=1100s.

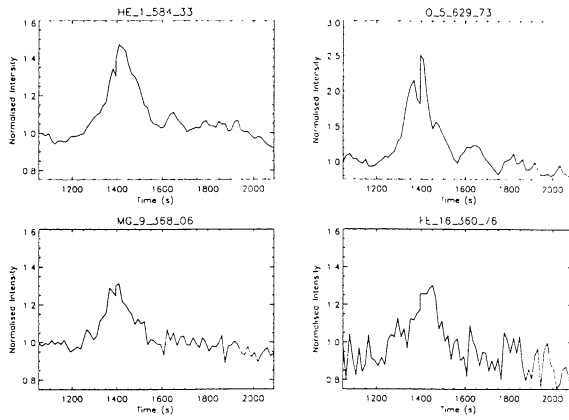


Figure 3. Event 1: normalised intensity (photons $\text{cm}^{-2} \text{s}^{-1} \text{arcsecs}^{-2}$) time history, relative to intensity at time=1100s, summed over pixels 57 to 70 along the slit.

of the event along the slit corresponds to approximately 15Mm.

To examine this particular event in greater detail, Figure 3 plots a time intensity curve for the summed intensity across pixels 57 to 70. The intensity has been normalised with regard to the intensity at time=1100s.

The O V curve shows the greatest intensity variation, displaying an increase by a factor of 2.5. At the same time, He I intensity increases by almost 50% and there are definite enhancements in Mg IX and Fe XVI as well. The He I and O V events rise to their maximum intensity in approximately 200s and decay in approximately 400s. It should be noted that the O V event rise phase begins slightly earlier than the corresponding increase in the other lines. Also, there is a sudden ‘dip’ at about 1400s for He I, Mg IX and Fe XVI which appears more significant in O V. A second post-event increase at 1650s is clearly visible in the chromospheric and transition region lines but not so much in the coronal ones.

As indicated in Section 1., a wide range of transient events have been detected in either UV, EUV or X-rays. In this case, we have detected an impulsive event that affects the plasma temperature over two orders of magnitude from the chromosphere through to the corona. It is possible to calculate an order of magnitude estimate for the energy content of this event for each particular temperature (see Harrison, 1997). Considering the typical temperature and density profiles with height as given in the literature, a cylindrical slab geometry is used for a blob of plasma at a certain temperature. The width of the slab is taken to be 1Mm so as to remain within a given region of the solar atmosphere (chromosphere, transition region or corona) while the maximum length along the slit which is brightened by the event corresponds to the diameter of the cylinder. Thus assuming a typical density value for a given temperature, the thermal energy content can be calculated - see Table 1.

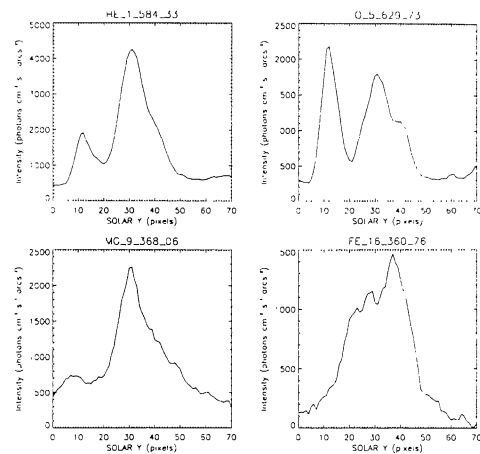


Figure 4. Event 2: intensity variation along the slit for all lines at time=340s in data s5763.

The energy content at O V is similar to blinkers: however, it should be noted that Harrison (1997) uses a different geometry than that described above. The Mg IX and Fe XVI lines indicate that the energy content in the ‘coronal’ event is of the order of nanoflares.

The Doppler velocity and line width profiles for both He I and O V seem to exhibit a degree of correlation over the range indicated. At $t = 1000\text{s}$ in He I, the red-shifted Doppler velocity increases from about 25kms^{-1} , to 32kms^{-1} at $t = 1400\text{s}$. In the meantime, the line width has increased from about 0.212\AA to 0.217\AA . For O V, it is interesting to note that the red shifted Doppler velocity decreases from 50kms^{-1} to 35kms^{-1} in the same time period, while the line width increases. It appears that the He I plasma is speeding up while the O V plasma is slowing down. If formation temperatures are related to solar atmosphere height (as is commonly assumed) then this may indicate the presence of an explosive event occurring between the chromosphere and the transition region. If we assume the material is ejected equally in all directions, then the ejected material slows down the plasma draining down from the transition region, and accelerates material already falling.

It appears that there is nothing to distinguish either the line width or Doppler velocity in both Mg IX and Fe XVI from either pre- or post-event times (if we take the event intensity maximum located at about $t = 1400\text{s}$). Table 1 has a summary of the plasma response to Event 1 in all the observed lines.

3.2. Event 2 (s5763 data)

Not long after the observations have started, a strong brightening occurs at the northernmost portion of the slit (solar y pixels 0 to 25) very close to an area of high intensity - see Figure 4 for event position. A summed intensity curve across pixels 7 to 17 normalised against the intensity at $t = 0$ is shown in

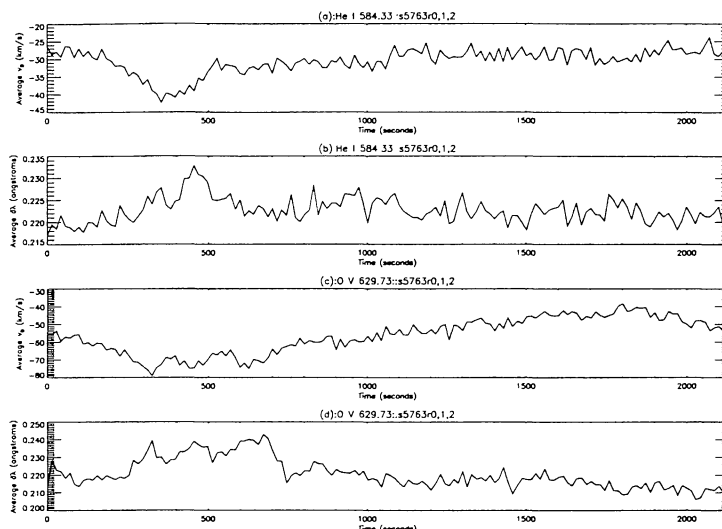


Figure 6. Event 2: measured Doppler velocities and line widths. (a) Space averaged Doppler velocity in He I for Event 2. (b) Space averaged line width in He I for Event 2. (c) Space averaged Doppler velocity in O V for Event 2. (d) Space averaged line width in O V for Event 2. All quantities average over the solar Y pixel range $7 \rightarrow 17$.

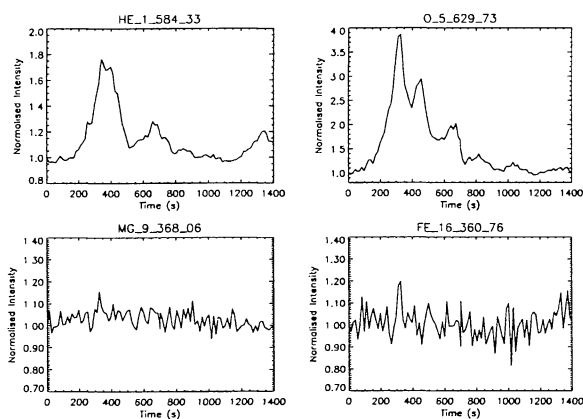


Figure 5. Event 2: normalised intensity ($\text{photons cm}^{-2} \text{s}^{-1} \text{arcsec}^{-2}$) (relative to intensity at time=0) time history summed over pixels 7 to 17 along the slit.

Figure 5. This transient event is very pronounced in He I (an increase of 80% on the “background” value) and O V (by a factor of nearly four) and there are indications of enhanced emission in the coronal lines at around the same time. The initial increase in the O V event begins earlier than the He I event and the O V curve has a very distinct “double peak”. In both He I and O V, a secondary intensity rise can be seen after 600s. This O V rise occurs slightly earlier than in He I. Mg IX and Fe XVI show little evidence for variations linked with this secondary feature. For the O V curve, the growth time to maximum intensity is approximately 360s, and about 800s later, the summed intensity has returned to a value comparable to that before the intensity increase occurred.

The He I Doppler velocity (see Figure 6(a)) has an interesting profile over the observation time. At $t = 0 - 100\text{s}$, the red shifted Doppler velocity is about 26km s^{-1} and quickly increases to about 40km s^{-1} at time $t = 0 - 100\text{s}$. It then falls again to about 26km s^{-1} at time $t = 600\text{s}$, which appears to be the background level. This peak in Doppler velocity coincides with the intensity peak seen in He I (Figure 5). Additionally, the line width behaviour (Figure 6(b)) appears to be correlated with both the intensity and Doppler velocity behaviour. The minimum line width, $\delta\lambda \approx 0.214\text{\AA}$, occurs at about $t = 100\text{s}$, which then rises to a maximum of about $\delta\lambda \approx 0.227\text{\AA}$ at $t = 450\text{s}$. The post-event intensity rise is not seen in either Doppler velocity or line width.

In O V, a similar type of behaviour is seen (Figure 6(c) and 6(d)). At $t = 0$, the red shifted average Doppler velocity is about 52km s^{-1} , which increases to $v_D \approx 76\text{km s}^{-1}$ at $t = 350\text{s}$. Simultaneously, the line width moves from $\delta\lambda \approx 0.215\text{\AA}$ to $\delta\lambda \approx 0.234\text{\AA}$. From these maximum values, the Doppler velocity and line width decrease to their approximate initial

values by about $t = 900$ s. For both lines, there appears to be a positive correlation between the line width and Doppler velocity.

Repeating the energy content calculation outlined in the previous Section, Table 1 contains a summary of Event 2 from the LOOPS_3 lines.

4. CONCLUSIONS

We have identified two isolated brightenings in the LOOPS_3 data which have been characterised by their duration, maximum lengthscale, possible energy deposition and calculated Doppler velocities (see Table 1). The greatest variation in intensity occurs in the O V line (2×10^5 K). Both Innes *et al* (1997) and Harrison (1997) find this to be the case in their bi-directional jets and blinkers respectively. The velocities found in each line in Event 1 and 2 lie in overlapping ranges, giving some measure of confidence that these are in fact examples of the same type of event. Additionally, the low temperature He I and O V lines have Doppler velocities commensurate with those estimated by Harrison 1997. However, it must be pointed out that Harrison 1997 emphasizes the questionable nature of this value of the Doppler velocity, caused by the low spectral resolution in the parent data.

The O V light curves obtained (see Figures 3 and 5) are redolent of those presented by Brekke, Fludra and Harrison 1997 in the same line. Given this, it seems reasonable to suggest that the Mg IX 368.06 Å and Fe XVI 360.76 Å light curves (Figure 3) are the higher temperature, short timescale counterparts to the events seen by Brekke, Fludra and Harrison 1997 and Harrison 1997.

Events 1 and 2 seem to ‘appear’ first in O V. Thus, one possibility is that some mechanism is heating more material to this particular temperature which is then seen slightly later in the lower (He I) and higher (Mg IX, Fe XVI) regions. This may indicate that the deposition of energy is occurring initially in the transition region which is then “conducted” in some sense to the chromosphere and corona. It may be that this energy transfer then triggers a large heating event in the chromosphere and a smaller one in the corona. Note, however, from our rough energy calculations that the energy content for the He I line is two orders of magnitude greater than that for the O V line. If the event originates in the chromosphere, a small transfer of this energy to the transition region (of 1 to 2 % say) would produce a much greater response in the OV line than in the He I line as the density in the transition region is much lower. The change in O V may then be “seen” first before any significant change in He I. Subsequently, the effect would then be “passed” onto the coronal lines.

The fact that Event 1 clearly affects plasma to coronal values (up to 2.5×10^6 K) presents us with the possibility that this brightening could be picked up by SXT on Yohkoh. From the Fe XVI line, there are indications that this event may be at the lower end of the ARTB range. Shimizu (1995) states that the transient brightenings observed by SXT may only be part of a much wider range of energy events. Event

1 may be an example of this. It is very interesting to note that the calculated energy content is of the order of nanoflares.

Note should be taken of the post-event intensity rises in both cases (Figures 3 and 5). Similar features have been observed by flare observers (Schmieder *et al*, 1994) and also in the most intense blinker reported by Harrison (1997). Also, the range of blinker lifetimes can extend up to the several hundreds of seconds investigated here. Therefore, it is our conclusion that Events 1 and 2 are best described as “active region blinkers”- intense, localised brightenings close to or within active regions where the plasma responds over a wide range of temperatures (chromospheric to coronal). The energy content for these ARB’s is larger than for blinkers in the same geometry (see Section 3.1) noting that only the “thermal” energy would be visible with these observations.

It is clear that further observations of active regions are required to generalise the characteristics of ARBs.

ACKNOWLEDGMENTS

All would like to acknowledge the encouragement and friendliness of all those present at the Experimental Operations and Analysis Facilities at the Goddard Space Flight Centre, Greenbelt, Maryland, USA.

REFERENCES

- Brekke, P., Fludra, A. and Harrison, R. A., Sol. Phys., in press.
- Cargill, P.J., Ap.J., 422, 381
- Dere, K.P. Adv. Space Res., 14, 13
- Harrison, R.A., Sol. Phys., in press.
- Innes, D.E., Inhester, B., Axford, W.I. and Wilhelm, K., Nature, in press.
- Ireland, J., Walsh, R.W., Harrison, R.A. and Priest, E. R., these proceedings.
- Kopp, R.A. and Poletto, G., Ap.J., 418, 496
- Moore, R.T., Porter, J., Roumeliotis, G., Tsuneta, S., Shimizu, T., Sturrock, P.A. and Acton, L.W., *Proc. of Kofu Symposium*, NRO Report No360, 89
- Narain, U., and Ulmschneider, P., Space Sci. Rev., 54, 377
- Parker, E. N., Ap.J., 330, 474
- Porter, J.G., Fontenla, J.M. and Simnett, G.M., Ap.J., 438, 472
- Schmieder, B., Fontenla, J.m Tandberg-Hanssen, E. and Simnett, G.M., *Proc. of Kofu Symposium*, NRO Report No360, 339
- Shimizu, T., PASJ, 47, 251-263.
- Vlahos, L., Georgoulis, M., Kluiving, R. and Paschos, P., A.&A., 299, 897-911.
- Walsh, R.W., Bell, G.E. and Hood, A.W., Sol. Phys., 171, 81
- Zirker, J.B., Coronal heating, Sol. Phys., 148, 43